Surface-plasmon-induced optical magnetic response in perforated trilayer metamaterial

T. Li,* H. Liu, F. M. Wang, J. Q. Li, Y. Y. Zhu, and S. N. Zhu†
National Laboratory of Solid State Microstructures, Nanjing University, Nanjing 210093, People's Republic of China
(Received 8 March 2007; revised manuscript received 14 April 2007; published 23 July 2007)

Surface plasmon excitations and the associated optical transmission properties in perforated metal/dielectric/metal trilayer structures are numerically investigated. Pronounced magnetic modes are observed in the antisymmetric and asymmetric modes of surface plasmon polaritons (SPPs). The influence of substrates on the magnetic response is studied in detail. Quite different from the conventional *LC*-circuit resonance, these magnetic excitations arise from the nonlocalized SPPs in the perforated layered structure, which may considerably enrich the electromagnetic properties of such metamaterials, especially the artificial magnetism at optical frequency.

DOI: 10.1103/PhysRevE.76.016606 PACS number(s): 41.20.Jb, 73.20.Mf, 42.25.Bs

Artificial materials, or so-called metamaterials, have recently sparked considerable interest, due mostly to their ability to exhibit designed electromagnetic (e.m.) responses not available in natural materials (such as negative refraction) [1]. Unlike the dielectric response for common optical materials, the magnetic response is rather difficult to access, because it always tails off at microwave frequency. Nevertheless, this limitation was overcome by an artificial design, the split-ring resonator (SRR) [2], whose magnetic response comes from an equivalent *LC*-circuit resonance. Since then, there have been sustained efforts to push the magnetic response to higher frequencies [3–5]. Until now, artificial nanoassemblies have been constructed to exhibit magnetism even at visible frequencies [6,7]. However, most of these designs are based on the *LC*-circuit resonance, which is considered inevitably to become saturated [8]. More recently, an optical magnetic response from a parallel plate metamaterial was reported, which is considered to come from a virtual current loop (VCL) [9]. In a former similar system of two parallel metallic wires, the researchers found that a magnetic mode can be excited by an antiparallel current via an antisymmetric surface plasmon polariton (SPP) mode in metal wires [10,11]. Here, we suppose that two perforated metal films should also accommodate an antisymmetric SPP mode that leads to a more efficient VCL for producing a magnetic response. So, in this paper, we numerically investigate the SPP modes and the associated magnetic excitations in a well-designed trilayer metamaterial [12]. Unlike recent studies of the negative refraction property arising from the *LC* circuit [12,13], we mainly care about the SPP-associated magnetic response; and the influence of the substrates is emphatically studied here, as it plays an important role in SPP excitations [14,15], and also in the magnetic responses.

We start our simulation on a structure containing a square array of square holes as shown schematically in Fig. 1, with the period $P=600$ nm, hole size $a=250$ nm, metal thickness $t=40$ nm, and separation $s=60$ nm. For diversity, our first sample (sample *A*) is defined as in a vacuum background (vacuum substrates and separation). In subsequent simulations, the separation is defined as SiO_2 with $\varepsilon=2.25$ $(n=1.5)$, while the substrates are defined as SiO_2 in turn (both vacuum for sample *B*, one SiO_2 for sample *C*, both SiO_2 for sample *D*). The metal is taken as gold with Drude dispersion ($\omega_p=1.37\times10^{16}$ rad/s and $\gamma=12.24\times10^{13}$ rad/s), where γ is set as three times the bulk one, as interpreted in Ref. [12].

CST MICROWAVE STUDIO, a finite-difference time-domain method based electromagnetic mode solver, is used in the numerical simulations. An incident plane wave with *y* polarization is placed so as to irradiate the four-unit-cell samples, which is defined to have periodic boundary conditions in the *x* and *y* directions, representing an infinite-periodic structure. Using the solver, a steady spatial distribution of the e.m. field within a certain frequency range can be provided after the simulation meets convergence, which is set as −60 dB here. Furthermore, by putting the structure into a waveguide with perfect *H* and perfect *E* conditions on the *x* and *y* boundaries, respectively, which is equivalently valid in an infinite-periodic structure for polarized incidence [16,17], we can obtain the transmission and reflection properties by evaluat-

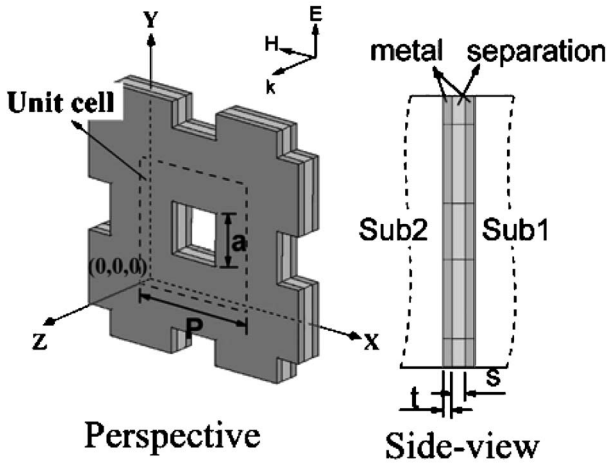

FIG. 1. Schematic of the perforated trilayer structure with four unit cells. The unit cell and the corresponding structural parameters are labeled: hole size *a*, period *P*, metal thickness *t*, and dielectric separation *s*. In the side view, "Sub1" and "Sub2" represent two substrates.

*Corresponding author. litao@nju.org.cn
†Corresponding author. zhusn@nju.edu.cn

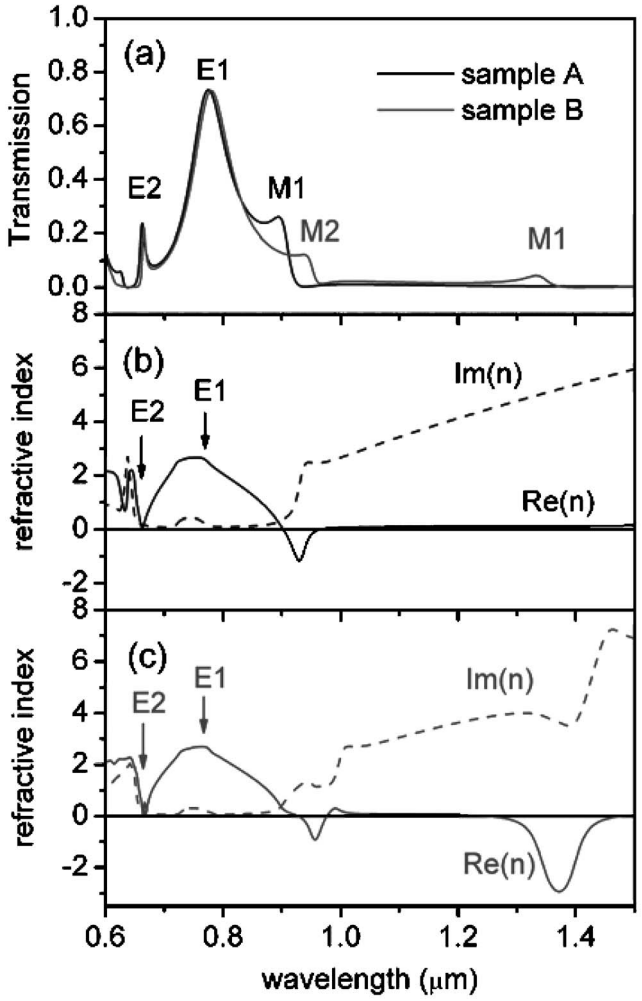

FIG. 2. Calculated transmission spectra of samples *A* and *B*, where *M*1 and *M*2 are magnetic modes arising from the *LC*-circuit resonance, while *E*1 and *E*2 are the SPP modes. (b), (c) Retrieved refractive indices for samples *A* and *B*, respectively, where the solid lines are the real part and dashed lines are the imaginary part.

ing the waveguide's *S* parameters. Three probes $(P1,P2,P3)$ are placed inside the gap with the locations of $(P/2,0,0)$, $(0,0,0)$, and $(0,P/2,0)$, respectively, in order to detect the local magnetic field.

First, we demonstrate the calculated transmission spectra of the samples *A* and *B* [see Fig. 2(a)]. It is clearly observed that two prominent transmission peaks located at about 0.66 and 0.78 μm are almost superposed (*E*1 and *E*2); while the spectral features at longer wavelength are rather different—only one peak for sample *A* (black, *M*1) but two peaks for sample *B* (gray, *M*1 and *M*2). In fact, peak *M*1 for both samples has the same origins—the well-recognized magnetic response leading to negative refraction, as is interpreted in detail in the work of Zhang *et al.* [12]. Because it comes from the *LC*-circuit resonance directly excited by the magnetic field of the incident wave, we call it a "magnetic polariton" [17]. The peak shift of the two samples is due to their different resonant frequencies, which are related to their effective capacitances and so to the permittivity of the medium inside the gap. As for the peak *M*2 of sample *B*, it is proved

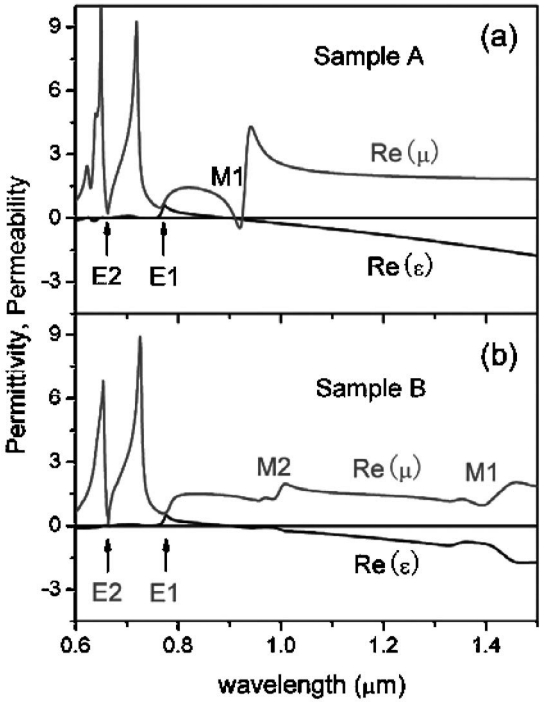

FIG. 3. Retrieved effective permittivity and permeability of (a) sample *A* and (b) sample *B*, in which corresponding modes *M*1, *M*2, *E*1, and *E*2 are marked.

to be another magnetic response, which also can lead to negative refraction. This is verified by the retrieved effective refractive index for these two samples [Fig. 2(b) for sample *A* and Fig. 2(c) for sample *B*] following the method in Ref. [18]. The negative refraction property of mode *M*1 agrees well with the original work [12]. For the *M*2 mode, detailed investigations suggest that it is related to a higher-order magnetic plasmon polariton mode associated with the hole array structure, which will not be intensively discussed here [19]. What interested us mostly for the moment is the two prominent modes *E*1 and *E*2, which are almost unaffected by changing the medium of the middle layer (both the spectrum and effective *n*). By careful observation of the retrieved Re(*n*) and Im(*n*) of samples *A* and *B*, we find that mode *E*1 reveals a normal positive refractive index with small loss, exhibiting a strong transmission in the spectrum; while, for mode *E*2, Re(*n*) goes down to a minimum (almost zero), though it does not reach a negative value. The analogous feature of *n* of mode *E*2 compared with modes *M*1 and *M*2 presumably indicates that *E*2 also corresponds to a magnetic response for both samples *A* and *B*. Along with the retrieved refractive index, we also obtained the effective permittivity and permeability as shown in Fig. 3. Great changes in magnetic permeability are found around the *E*2 mode, as well as the *M* modes for both samples, indicating strong magnetic excitations. Apparently, the *E*2 mode is rightly located at a sharp dip of permeability and *E*1 at a peak of permittivity, indicating the magnetic and electric excitations, respectively. As a result of the relative good match between the permittivity and permeability at these two modes, the transmission reaches two local maxima.

Another way to check the magnetic excitation is to detect

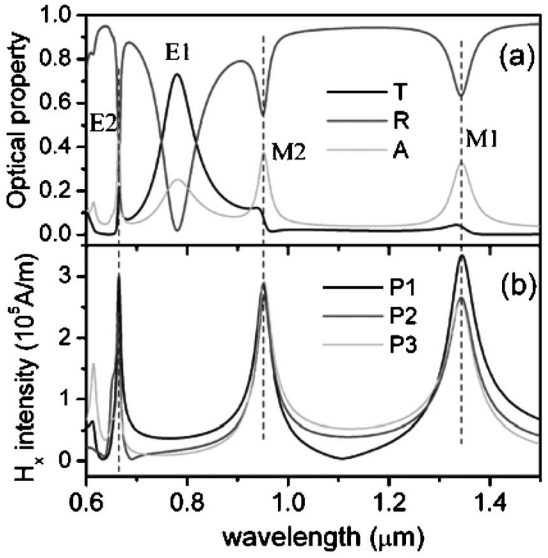

FIG. 4. (a) Transmission (black), reflection (gray), and absorption (light gray) spectra of sample B. (b) Local magnetic field (H_x) detected by three probes.

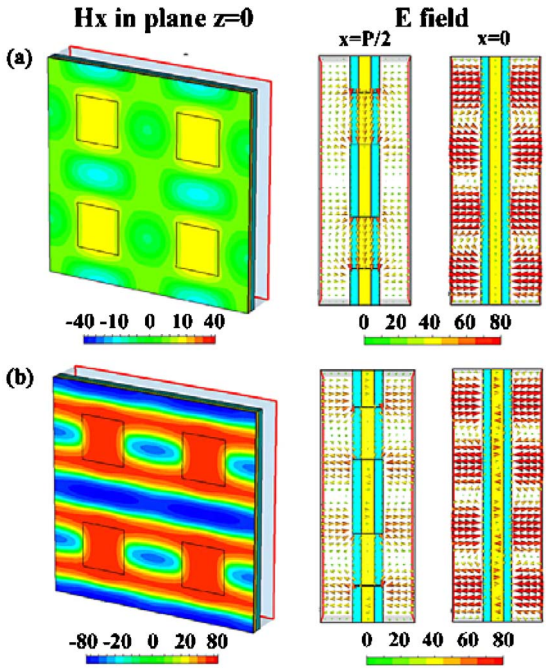

FIG. 5. (Color online) Magnetic field (H_x) map in xy-cut plane ($z=0$), and electric field distributions in yz-cut planes ($x=P/2$ and $x=0$) for (a) mode $E1$ and (b) mode $E2$ of sample B.

the local field inside the gaps. Figure 4(a) redisplays the transmission spectrum of sample B accompanied by the reflectance and absorptance, and Fig. 4(b) shows the corresponding local magnetic field (H_x) detected by three probes. One can easily find that the total four transmission peaks correspond to the local reflection minimum and absorption maximum. However, from the detected magnetic field, only three H_x enhancements are observed in modes $M1$, $M2$, and $E2$. As mentioned above, $M1$ and $M2$ belong to the "magnetic polariton" modes, where strong magnetic resonance occurs. As for $E1$ and $E2$, they are very similar to the doublet transmission features in previous studies of the SPPs in single metallic films with symmetric dielectric substrates, which is considered to come from the coupling of the SPPs excited on both metal surfaces [15,20]. But, interestingly, why does only one mode ($E2$) exhibit magnetic field enhancement in our case? To get a clear understanding, the H_x field map in the gap (xy plane) and the electric field distributions in two typical yz planes (crossing and not crossing the holes) for the $E1$ and $E2$ modes are illustrated in Fig. 5 (the maximum value is selected). Apparently, the magnetic field in the mode $E1$ is much weaker than that in $E2$, which agrees well with the result of the detected H_x. By inspecting the corresponding electric field, we find that $E1$ and $E2$ truly correspond to two characteristic modes—symmetric and antisymmetric, respectively. Furthermore, the field intensity in the continuous parts ($x=0$) is stronger than in the fractional parts ($x=P/2$), indicating more contributions from the SPP-induced surface wave than from the localized resonance inside the holes. From Fig. 5, we realize that E_z inside the gap is almost counteracted for the symmetric mode, while for the antisymmetric mode considerable E_z remains to build VCLs, and thus a strong magnetic response is excited.

To check the influence of the substrates, we simulate the sample C, one of whose substrates is changed to SiO_2. It is actually the most popular case in experimental approaches [12,13]. Figures 6(a) and 6(b) show the transmission spectrum and the detected H_x intensities, respectively. With careful observation, we find that, although the spectrum appears quite different from that of sample B, the peaks $M1$ and $M2$ remain unchanged. This confirms the conclusion from the magnetic polariton modes, whose resonant frequency is determined by the effective LC character. However, the SPP excitation strongly depends on the dielectric substrate; the responses of $E1$, $E2$, and $E3$ are undoubtedly attributed to the excited SPPs. According to the excitation condition of SPP [21], we have the SPP-enhanced transmission maximum approximately at [22]

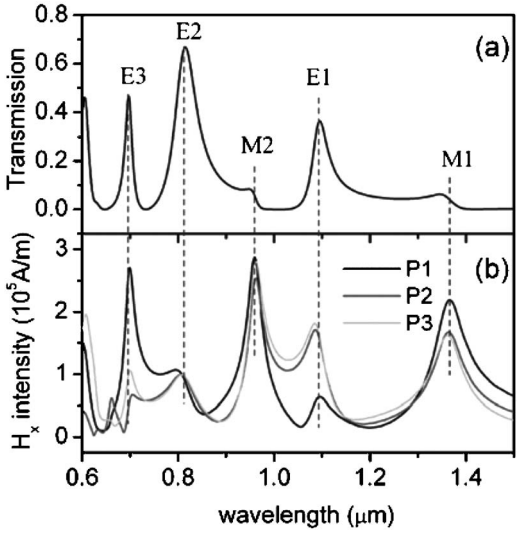

FIG. 6. (a) Transmission spectrum of sample C. (b) Local magnetic field (H_x) detected by three probes.

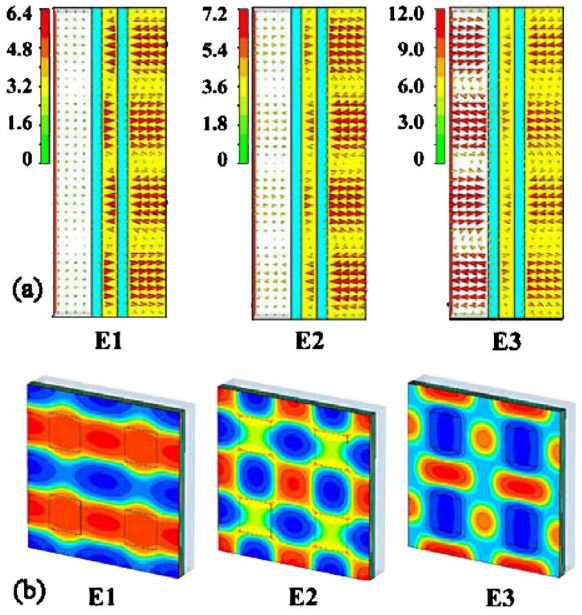

FIG. 7. (Color online) (a) Electric field distributions in *yz* plane ($x=0$) for three SPP modes $E1$, $E2$, and $E3$ of sample C. (b) Corresponding H_x maps in *xy*-plane ($z=0$).

$$\lambda_{SPP} = \frac{2\pi}{|G_{ij}|}\sqrt{\frac{\varepsilon_m \varepsilon_d}{\varepsilon_m + \varepsilon_d}}, \tag{1}$$

where ε_m and ε_d are the permittivity of the metal and dielectric, respectively, and G_{ij} is the reciprocal vector of the hole array. From Eq. (1), one has the relations

$$\frac{(\lambda_{SPP})_{sub1}}{(\lambda_{SPP})_{sub2}} = \sqrt{\frac{\varepsilon_m \varepsilon_{d1}}{\varepsilon_m + \varepsilon_{d1}}}\sqrt{\frac{\varepsilon_m + \varepsilon_{d2}}{\varepsilon_m \varepsilon_{d2}}} \approx \frac{n_{d1}}{n_{d2}} \tag{2a}$$

for two modes with the same reciprocal vectors, and

$$\frac{(\lambda_{SPP})_{G1}}{(\lambda_{SPP})_{G2}} = \frac{|G_2|}{|G_1|} \tag{2b}$$

for two modes excited at the same metal/dielectric interfaces. As for the new modes in sample C, the peak $E1$ is redshifted to about 1.5 times the average position of the previous coupled SPPs for sample B, suggesting a SPP mode on the Au/SiO_2 interface as the n_{SiO_2} is set at 1.5 times the vacuum. However, peaks $E2$ and $E3$ appear a little inexplicable. To definitely characterize these peaks, we still refer to the field distributions. Figure 7(a) shows the electric field distributions in the *yz* plane of $x=0$ of the three modes, from which the SPP modes are clearly distinguished; we see that $E1$ and $E2$ belong to the SPPs on the Au/SiO_2 interface, and $E3$ to the Au/vacuum interface. More careful inspection of the H_x maps in the *xy* plane [shown in Fig. 7(b)] indicates that modes $E1$ and $E2$ actually correspond to the SPP excitations associated with the reciprocal vectors of $G_{1,0}$ and $G_{1,1}$, respectively. In any case, the SPP excitations for these three modes are asymmetric, and a net E_z field remains inside the gaps and forms VCLs, which surely leads to the magnetic responses. As a result of the counteraction, these magnetic responses from the asymmetric modes are weaker than the antisymmetric mode of the coupled case.

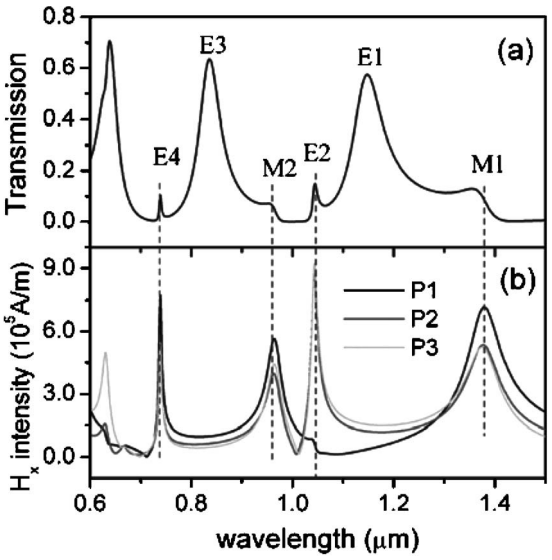

FIG. 8. (a) Transmission spectrum of sample D. (b) Local magnetic field (H_x) detected by three probes.

Furthermore, sample D with both SiO_2 substrates is also investigated with the transmission spectrum and detected local field shown in Fig. 8. Comparing it with that of sample B (Fig. 4), we find that the first two SPP modes ($E1$ and $E2$) are both pushed to longer wavelengths, and new modes ($E3$ and $E4$) emerge. Evaluating these mode positions, we obtained that $(\lambda_{E1})_D/(\lambda_{E1})_B \approx 1.49$, $(\lambda_{E2})_D/(\lambda_{E2})_B \approx 1.56$, $(\lambda_{E1})_D/(\lambda_{E3})_D \approx 1.38$, and $(\lambda_{E2})_D/(\lambda_{E4})_D \approx 1.41$. Since n_{SiO_2} is 1.5 times n_{vac}, $(\lambda)_D/(\lambda)_B \approx 1.5$ agrees with Eq. (2), which confirms that $E1$ and $E2$ belong to the coupled SPP modes on the two Au/SiO_2 interfaces. Also, $(\lambda_{E1,E2})/(\lambda_{E3,E4}) \approx 1.41$ agrees well with $|G_{1,1}| \approx 1.41|G_{1,0}|$ (for a square lattice); $E3$ and $E4$ are proved to be the coupled $G_{1,1}$ modes of the SPP. As expected, the antisymmetric modes $E2$ and $E4$ exhibit strong magnetic responses, as the detected local magnetic field shows.

From the above analysis, we realize that the magnetic response can be excited not only by the *LC*-resonance-induced "magnetic polariton," but also by the SPP-excited VCLs in layered structures. Because this kind of magnetic response mainly depends on the surface plasmon excitations, it is expected to be more convenient to manipulate the metamaterial's optical properties by modifying the metal surfaces. As the present results show, some of the magnetic responses are well located at the visible frequency, and they also can be pushed to higher frequencies by adjusting the structural parameters.

In summary, we have numerically demonstrated pronounced magnetic modes associated with extraordinary optical transmissions in perforated metal/dielectric trilayer structures. By alternating the dielectric substrates, we find that the magnetic responses exist in the antisymmetric and asymmetric modes for the same and different substrates, respectively.

These magnetic modes inherit the characteristics of the well-known SPPs (e.g., higher modes), indicating more selectivity in designing specific metamaterials with preferred e.m. responses. Moreover, this finding provides a method to generate strong magnetic responses at optical frequencies, which no longer relies on the traditional *LC*-circuit resonance.

This work is supported by the China Postdoctoral Science Foundation (Grant No. 2006390928), the National Natural Science Foundation of China (Grants No. 10534020, No. 10474042, No. 10604029, and No. 10523001), and by the State Key Program for Basic Research of China under Grant No. 2006CB921804.

[1] D. R. Smith, J. B. Pendry, and M. C. K. Wiltshire, Science **305**, 788 (2004).
[2] J. B. Pendry, A. J. Holden, D. J. Robbins, and W. J. Stewart, IEEE Trans. Microwave Theory Tech. **47**, 2075 (1999).
[3] R. A. Shelby, D. R. Smith, and S. Schultz, Science **292**, 77 (2001).
[4] T. Y. Yen, W. J. Padilla, N. Fang, D. C. Vier, D. R. Smith, J. B. Pendry, D. N. Basov, and X. Zhang, Science **303**, 1494 (2004).
[5] C. Enkrich, M. Wegener, S. Linden, S. Burger, L. Zschiedrich, F. Schmidt, J. F. Zhou, Th. Koschny, and C. M. Soukoulis, Phys. Rev. Lett. **95**, 203901 (2005).
[6] A. N. Grigorenko, A. K. Geim, H. F. Gleeson, Y. Zhang, A. A. Firsov, I. Y. Khrushchev, and J. Petrovic, Nature (London) **438**, 335 (2005).
[7] T. Pakizeh, M. S. Abrishamian, N. Granpayeh, A. Dmitriev, and M. Kall, Opt. Express **14**, 8240 (2006).
[8] J. Zhou, Th. Koschny, M. Kafesaki, E. N. Economou, J. B. Pendry, and C. M. Soukoulis, Phys. Rev. Lett. **95**, 223902 (2005).
[9] Z. M. Huang, J. Q. Xue, Y. Hou, J. H. Chu, and D. H. Zhang, Phys. Rev. B **74**, 193105 (2006).
[10] V. A. Podolskiy, A. K. Sarychev, and V. M. Shalaev, Opt. Express **11**, 735 (2003).
[11] V. A. Podolskiy, A. K. Sarychev, E. E. Narimanov, and V. M. Shalaev, J. Opt. A, Pure Appl. Opt. **7**, S32 (2005).
[12] S. Zhang, W. Fan, N. C. Panoiu, K. J. Malloy, R. M. Osgood, and S. R. J. Brueck, Phys. Rev. Lett. **95**, 137404 (2005).
[13] G. Dolling, C. Enkrich, M. Wegener, C. M. Soukoulis, and S. Linden, Science **312**, 892 (2006).
[14] T. W. Ebbesen, H. J. Lezec, H. F. Ghaemi, T. Thio, and P. A. Wolff, Nature (London) **391**, 667 (1998).
[15] L. Martin-Moreno, F. J. Garcia-Vidal, H. J. Lezec, K. M. Pellerin, T. Thio, J. B. Pendry, and T. W. Ebbesen, Phys. Rev. Lett. **86**, 1114 (2001).
[16] M. Beruete, M. Sorolla, and I. Campillo, Opt. Express **14**, 5445 (2006).
[17] T. Li, H. Liu, F. M. Wang, Z. G. Dong, S. N. Zhu, and X. Zhang, Opt. Express **14**, 11155 (2006).
[18] D. R. Smith, D. C. Vier, T. Koschny, and C. M. Soukoulis, Phys. Rev. E **71**, 036617 (2005).
[19] T. Li, J. Q. Li, F. M. Wang, Q. J. Wang, H. Liu, S. N. Zhu, and Y. Y. Zhu, Appl. Phys. Lett. **90**, 251112 (2007).
[20] A. Benabbas, V. Halte, and J.-Y. Bigot, Opt. Express **13**, 8730 (2005).
[21] Q. J. Wang, J. Q. Li, C. P. Huang, C. Zhang, and Y. Y. Zhu, Appl. Phys. Lett. **87**, 091105 (2005).
[22] Although many researchers found that enhanced transmission positions always diverge from the calculated SPP excitations on a flat metal surface due to composite attributions, such as SPPs, cavity plasmon resonance, evanescent wave diffraction, and so on, the SPP still plays an important role. So, to simplify interpretation, we define all these *E* modes as SPP modes.